Environmental Science
Water Research & Technology

Antifouling UV-treated GO/PES Hollow fiber membrane in membrane bioreactor (MBR)

Journal:	*Environmental Science: Water Research & Technology*
Manuscript ID	EW-ART-03-2019-000217.R1
Article Type:	Paper
Date Submitted by the Author:	16-Apr-2019
Complete List of Authors:	Fathizadeh, Mahdi; University of South Carolina, Catalysis for Renewable Fuels Center Department of Chemical Engineering Xu, Weiwei; Rensselaer Polytechnic Institute Department of Chemistry and Chemical Biology, Department of Chemistry and Chemical Biology Shen, Margaret; Montgomery Blair High School Jeng, Emily ; Cornell University Zhou, Fanglei ; Rensselaer Polytechnic Institute, DONG, QIAOBEI; Rensselaer Polytechnic Institute, Behera, Dinesh; Rensselaer Polytechnic Institute Department of Chemistry and Chemical Biology song, zhuonan; University of South Carolina, Chemical Engineering Wang, Lei; University of South Carolina Shakouri, Abolfazl; University of South Carolina Khivantsev, Konstantin; University of South Carolina, Chemical Engineering Yu, Miao; Rensselaer Polytechnic Institute, Chemical and Biological Engineering

Water impact statement

Membrane bioreactor (MBR), which utilizes membranes for water filtration from activated sludge, are being widely investigated as an effective method for municipal and industrial wastewater treatment. Current membranes, however, are easily clogged by accumulation of activated sludge on membrane surface and/or in pores, and thus suffer from severe membrane fouling problem, which significantly shortens the lifespan of the membranes and also increases operation cost due to frequent cleaning. It is, therefore, in a great need to develop antifouling membranes for highly efficient MBR application. Herein, Single layer graphene oxide (SLGO) was studied as a novel coating material to drastically improve antifouling performance of polyether sulfone (PES) hollow fiber (HF) membrane in membrane bioreactor (MBR) application. By selectively modifying membrane surface, only small amount of SLGO coating (6.2 mg/m^2) was needed to achieve acceptable membrane performance. The UV treatment on SLGO coating was further assisted to improve antifouling properties of as-prepared PES HF membranes.

ARTICLE

Antifouling UV-treated GO/PES Hollow fiber membrane in membrane bioreactor (MBR)

Mahdi Fathizadeh[a#], Weiwei L. Xu[b#], Margaret Shen[c#], Emily Jeng[d#], Fanglei Zhou[b], Qiaobei Dong[b], Dinesh Behera[b], Zhuonan Song[a], Lei Wang[a], Abolfazl Shakouri[a], Konstantin Khivantsev[a], and Miao Yu[b]*

Received 00th January 20xx,
Accepted 00th January 20xx

DOI: 10.1039/x0xx00000x

Single layer graphene oxide (SLGO) was studied as a novel coating material to drastically improve antifouling performance of polyether sulfone (PES) hollow fiber (HF) membrane in membrane bioreactor (MBR) application. By selectively modifying membrane surface, only small amount of SLGO coating (6.2 mg/m^2) was needed to achieve acceptable membrane performance. The UV treatment on SLGO coating was further assisted to improve antifouling properties of as-prepared PES HF membranes. By comparing the transmembrane pressure of pristine PES HF and PES_$GO_{6.20}$_UV_X (X = 0-1.5 h) membranes in MBR for wastewater treatment at a fixed water flux, the PES_$GO_{6.20}$_$UV_{1.0}$ membrane coated with 1 h UV-treated SLGO was demonstrated to substantially relieve bio-fouling problem. To understand the influence of SLGO modification on membrane performance, FESEM, ATR-FTIR, and AFM analyses were conducted to characterize as-prepared membranes, and the SLGO deposition mechanism was also proposed in this study.

1. Introduction

Membrane bioreactor (MBR), which utilizes membranes for water filtration from activated sludge, are being widely investigated as an effective method for municipal and industrial wastewater treatment. Current membranes, however, are easily clogged by accumulation of activated sludge on membrane surface and/or in pores, and thus suffer from severe membrane fouling problem, which significantly shortens the lifespan of the membranes and also increases operation cost due to frequent cleaning [1-4]. It is, therefore, in a great need to develop antifouling membranes for highly efficient MBR application [5-7].

Among various membranes, polyether sulfone (PES) hollow fiber (HF) membranes have been widely studied in MBR application because of their low cost, excellent stabilities, facile fabrication process, and high surface to volume ratio [8-10]. Hydrophobic nature of PES, however, makes them more prone to foul. To improve the hydrophilicity of PES and thus its antifouling performance, hydrophilic nanomaterials, such as TiO_2, silica, graphene oxide (GO), and oxidized carbon nanotubes, have been employed as additives [7, 8, 11]. However, a relatively large amount of additives usually needs to be uniformly dispersed in the whole polymer membranes to obtain improved surface hydrophilicity. This not only increases the material cost, especially for expensive additives, but also potentially changes the mechanical stability of membranes. In

[a] *Department of Chemical Engineering, University of South Carolina, Columbia, SC 29208, USA.*
[b] *Department of Chemical and Biological Engineering, Rensselaer Polytechnic Institute, Troy, NY 12180, USA*
[c] *Science, Mathematics, and Computer Science Magnet Program, Montgomery Blair High School, 51 University Blvd E, Silver Spring, MD 20901, USA.*
[d] *School of Chemical and Biomolecular Engineering, Cornell University, Ithaca, New York 14853, United States*
#: Contribute equally
† Electronic Supplementary Information (ESI) available: AFM image *of* SLGO flakes; ATR-FTIR of SLGO, UV-treated SLGO, pristine PES HF and SLGO/UV-treated SLGO coated PES HF membranes; The pore size distribution of PES HF membranes; FESEM and AFM topological scan of PES HF membranes. See DOI: 10.1039/x0xx00000x

contrast, surface modification has been shown as an effective way to selectively modify membrane surface hydrophilicity. Comparing with various methods [12-17], depositing ultrathin hydrophilic coatings by facile solution phase deposition methods may effectively enhance membrane surface hydrophilicity while maintaining the bulk polymer characteristics [18, 19].

Recent years, GO has attracted lots of attention as a promising two-dimensional coating material, owing to its one carbon atom thickness, ease of conformation to substrates, excellent chemical stability, and mechanical strength [20-26,34]. Besides, it also has been tested as an effective additive to improve the antifouling performance of PES membranes. For example, Lee *et al*.[27] and Jin *et al*.[28] prepared mixed matrix membranes by uniformly mixing GO with PES for wastewater treatment and for oil/water separation. Their results indicated that GO significantly increased the hydrophilicity of PES membranes and substantially improved water flux [27]. However, a large amount of GO, around 2.5 wt.% relative to the polymer weight, was needed to obtain a significant improvement, with most of the GO flakes being embedded inside the PES membranes. Therefore, it would be highly desirable to selectively deposit GO flakes only on the PES membrane surface to drastically lower the amount of GO required to improve surface hydrophilicity. In addition, we found that UV treatment increased the O/C ratio in GO flakes and thus effectively improved hydrophilicity of GO coatings. Applying UV-treated GO coatings on PES may further improve the surface hydrophilicity [7, 28, 29]. Thus, herein, we first investigated effect of surface modification with GO coating on improving the antifouling performance of PES HF membranes in membrane bioreactor application. The anti-biofouling ability of GO deposited PES HF membranes were evaluated with both simulated foulants and activated sludge provide by local industry. Besides, since UV treatment for GO flakes is a facile way to increase the GO hydrophilicity, we also applied UV treated GO coating to improve the antifouling performance of PES HF membranes.

2. Materials and methods

2.1 Single layer GO (SLGO) dispersion preparation and coating deposition

PES HF (diameter: 6 mm) with molecular weight cutoff (MWCO) at around 150 KDa was purchased from Hydranautics–Nitto Group Company. The selective PES layer is on the external surface of the HF. SLGO was purchased from Cheap Tubes, Inc. (Brattleboro, VT, USA), and SLGO dispersion was prepared by the following procedure. One gram of SLGO was added in 1 liter of deionized water and subsequently sonicated for 2 h. After sonication, the SLGO dispersion was centrifuged at 8,000 rpm for 1 h to remove large aggregates and obtain SLGO dispersion. UV-vis spectrum of the SLGO dispersion was then measured, and the SLGO concentration in the as-prepared dispersion was determined by a calibration curve using standard GO dispersions. The obtained SLGO stock dispersion was appropriately diluted to obtain SLGO coating dispersion with a concentration of 1.91×10^{-4} mg/mL. UV lamp (B-100Y, Mineralogical Research Company) was used to treat the SLGO flakes to produce more hydrophilic SLGO. Specifically, SLGO dispersion was vigorously stirred under UV irradiation with different times.

A facile vacuum filtration method was used to deposit SLGO and UV-treated SLGO on PES HFs. Before filtration, one end of the PES HFs was sealed with epoxy, and the other end was connected to a vacuum pump. These HFs were then put into the SLGO and UV-treated SLGO dispersion for the filtration coating. The pressure drop across the membrane was fixed to 30 kPa. SLGO loading amount (mg/m^2) and UV treatment time for different membranes were listed in Table 1. SLGO coated PES HF membranes were dried under vacuum for 12 h at 60 °C before being used for filtration tests.

Table 1. Preparation and post treatment conditions for SLGO coated PES HF membranes.

Membrane	GO content (mg/m^2)	UV treatment time (h)
PES	0	0
$PES\_GO_{1.55}$	1.55	0
$PES\_GO_{3.10}$	3.10	0
$PES\_GO_{6.20}$	6.20	0
$PES\_GO_{9.31}$	9.31	0
$PES\_GO_{6.20}\_UV_{0.5}$	6.20	0.5
$PES\_GO_{6.20}\_UV_{1.0}$	6.20	1.0
$PES\_GO_{6.20}\_UV_{1.5}$	6.20	1.5

2.2 Membrane characterizations

Surface functional groups of SLGO (with and without UV treatment) coated PES HF membranes and uncoated PES HFs were characterized by Attenuated Total Reflection-Fourier Transform Infrared Spectroscopy (ATR-FTIR) analysis. ATR-FTIR spectra were collected on a Nicolet 6700 FTIR spectrometer (Thermo Scientific, Waltham, MA, USA) over the range of 800–4,000 cm^{-1}. Dried PES HF membranes were placed on a glass substrate, and then the laser beam was focused on the center of the membrane surface.

Surface morphologies and the pore sizes of PES HF membranes were examined with Field Emission Scanning Electron Microscope (FESEM) (Zeiss UltraPlus, Germany). The pore size distribution was calculated by ImageJ. Samples for the cross-sectional SEM images were prepared by immersing PES HF membranes in liquid nitrogen for several minutes, and then broke them into small rings with sharp edge. The surface roughness of pristine PES HFs and SLGO coated PES HF membranes was measured by Atomic Force Microscopy (AFM) (AFM Workshop, CA, USA), and average results from five measurements were reported.

2.3 Membrane filtration measurements

Membrane filtration performance was investigated by using PES HFs with a total filtration area of ~10 cm^2 in the MBR system

(Figure 1). During filtration measurements, PES HF membranes were directly submerged in the MBR reactor, and the total flux through HFs with and without the presence of foulants in the feed solution was determined under a constant pressure drop of around 30 kPa controlled by a vacuum pump and an adjustable venting needle valve. Continuous air flow was introduced using an air blower placed at the bottom of the liquid tank through an air diffuser. Air flow can remove solid accumulation on PES HF surface and supply required oxygen for the microorganisms. The SLGO coated PES HF membranes and uncoated HFs were tested for at least 4 h to obtain steady state results. Bovine serum albumin (BSA >98%, purchased from Sigma Aldrich), sodium alginate (SA), and silicon dioxide (SiO_2) particles were selected as model foulants to investigate the antifouling performance of the pristine PES HFs and SLGO coated PES HF membranes. Table 2 summarizes particle size of these foulants and concentration of foulant in the feed solution (top). The single-foulant filtration measurements were used to investigate the effect of SLGO loading and UV treatment time on antifouling properties of the PES HF membranes.

Table 2. The component of waste water for the fouling test and the condition for long term MBR reactor testing.

Wastewater content		
Foulants	Concentration (mg/L)	Particle Size (nm)
Bovine serum albumin	50	550
Sodium Alginate	50	240
Silicon dioxide particle	1000	1500
MBR reactor testing condition		
Reactor volume	1	liter
MLSS	8000	mg/L
Feed concentration (TOC)	2000	ppm
F/M ratio	0.2	-
pH	~7	
Membrane area	10	cm^2
Sludge source	Metropolitan Wastewater Treatment Plant, Columbia, SC, USA	

The optimized SLGO coated PES HF membrane was used for membrane MBR testing; during the test, constant flux operation mode was adopted, while the trans-membrane pressure was monitored (Figure 1). Constant permeation flux was controlled by adjusting the pressure of vacuum pump using a needle valve. The simulated wastewater was prepared by mixing 5 g/L of skim milk, 5 g/L of sucrose, 0.1 g/L of $MgSO_4$, and 0.1 g/L of NH_4Cl [30]. The activated sludge was provided by the City's Metropolitan Wastewater Treatment Plant (Columbia, SC, USA) with mixed liquor suspended solid (MLSS) concentration of 8,000 mg/L. In the designed MBR reactor, volume, aeration rate, permeation flux and food-to-microorganism (F/M) ratio were fixed at 1 L, 1 L/min, 20 L/(m^2·h) and 0.2, respectively. The operation condition of MBR reactor is given in Table 2 (buttom). Total organic carbon (TOC) analyzer was used to measure the concentration of carbon in both feed and permeate sides. TOC concentration was measured by two analyses: one to measure total carbon (TC), and the other to measure inorganic carbon (IC). The difference between these two measurements is rigorously TOC concentration. For this approach, 20 mL of MBR permeate was used for TOC analysis (Tekmar Phoenix 8000-Persulfate TOC Analyze). Reported TOC for each 4 h was tested for three times.

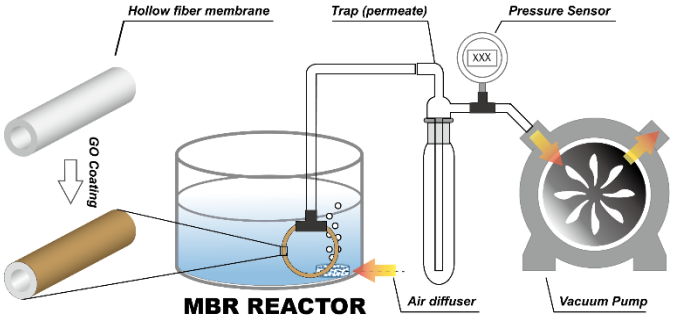

Figure 1. Schematic illustration of lab scale membrane bio-reactor (MBR).

3. Results and discussion

3.1 SLGO coatings on PES membrane surface

In this work, the SLGO dispersion was prepared through long term sonication, followed by high speed centrifugation. The single layer feature of as-prepared GO flakes was confirmed by AFM image shown in Figure S1a, and the lateral size of SLGO flakes was around 0.7-1.3 µm. Figure S1b exhibits the ATR-FTIR spectrum of SLGO dispersed in water; the characteristic peaks of -C=O, -C-OH (carboxyl functional groups) and C=C stretching were detected at 1,720, 1,430, and 1,540-1,620 cm^{-1}, corresponding well to the typically reported GO structure and indicating the presence of pristine graphic carbon and various hydrophilic functional groups on the SLGO flakes.

To fabricate SLGO deposited PES HF membranes, a facile vacuum filtration method was applied, and the detailed process was described in the materials and methods part. Since PES HF has small pores (~300 nm), medium pores (~860 nm) and large (~ 1,300 nm) pores that were split into smaller pores below the surface (see discussion for Figure 3 below), there might exist three sequential stages during the overall SLGO deposition process, as proposed schematically in Figure 2. In the first stage, SLGO is expected to deposit on the surface of small pores, diffuse to the inside of large pores, and partially cover the edge of medium pores. In the second stage, with increasing loading of SLGO, most of the membrane surface would be covered with SLGO flakes, which could increase hydrophilicity of the PES membrane. In this stage, the loading of SLGO should be optimized to generate the lowest mass transfer resistance while greatly improving the hydrophilicity of the

membrane surface. In the third stage, as the SLGO flakes keep staking on the PES membrane surface, the permeance of the membrane would decrease because of the increased transport resistance. In this work, we fabricated PES HF membranes with different loadings of SLGO and UV-treated SLGO (Table 1) and studied their influence on membrane separation performance and antifouling ability in MBR.

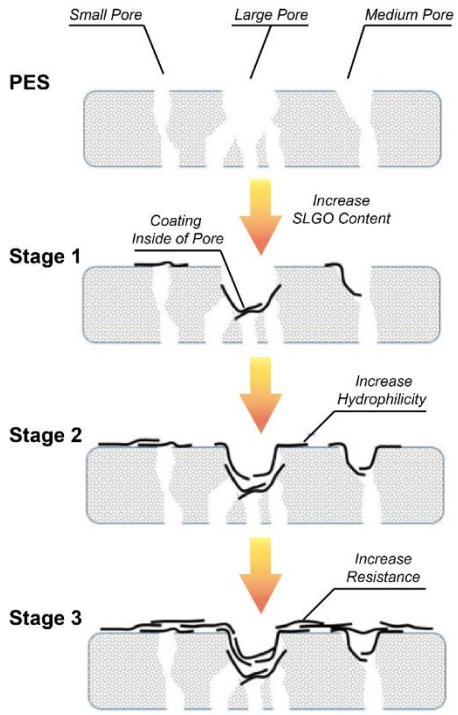

Figure 2. Proposed SLGO coating mechanism on PES hollow fiber membrane.

ATR-FTIR was first applied to characterize the pristine PES HF and SLGO coated PES HF membranes. As shown in Figure S2, the pristine PES HF had characteristic peaks at 1,578 and 1,485 cm^{-1}, which can be assigned to the aromatic C=C bond and C-C bond stretching. The phenyl ether bond of PES appeared at around 1,240 cm^{-1} and was observed in all membranes. Besides that, absorption peaks at 1,320 and 1,150 cm^{-1} were attributed to asymmetric and symmetric stretches of sulfone group (SO_2) in PES, which is consistent with the characterization results of PES membranes reported in the literature [15]. After SLGO coating, new peaks at 1,220, 1,540, 1,720, and 2,950 cm^{-1}, corresponding to epoxy, carboxyl, and aromatic functional groups of SLGO, were clearly observed. The relative intensity of carboxyl or epoxy groups to SO_2 group can reflect the increase of SLGO loading on the PES surface; with the increase of SLGO loading on PES HF from 1.55 to 9.31 mg/m^2, the ratio of carboxylic acid group to SO_2 group gradually increased.

FESEM was carried out to investigate the surface morphology of the pristine PES HF and SLGO deposited HF membranes (Figure 3). Figure 3A&B illustrates that PES HF had a continuous porous structure, and the HF surface had pores with size in the range from 0.2 to 1.7 µm. With the increase of SLGO loading on PES HF (Figure 3C-F), number of pores decreased and most of the smaller pores were covered with SLGO flakes. To further investigate the SLGO coating process, the FESEM were analyzed by ImageJ to obtain the trend of pore size distribution change with SLGO loading. As shown in Figure S3, the pristine PES HF had three pore size peaks located at 300, 860 and 1,300 nm. With the increase of SLGO loading, the small pores (300 nm) started to disappear; as SLGO loading increased to 3.1 mg/m^2, the small pores were totally covered, and the relative amount of medium pores (860 nm) started to drop; when the SLGO loading further increased to 6.2 and 9.31 mg/m^2, medium size pores were mostly covered, and the amount of uncovered large pores (1,300 nm) were reduced significantly. As a result, the extra-large pores (>1,500 nm) which account very small portions on pristine PES HF gradually played the dominant role, and the corresponding pore size distribution peak shifted to larger size as well.

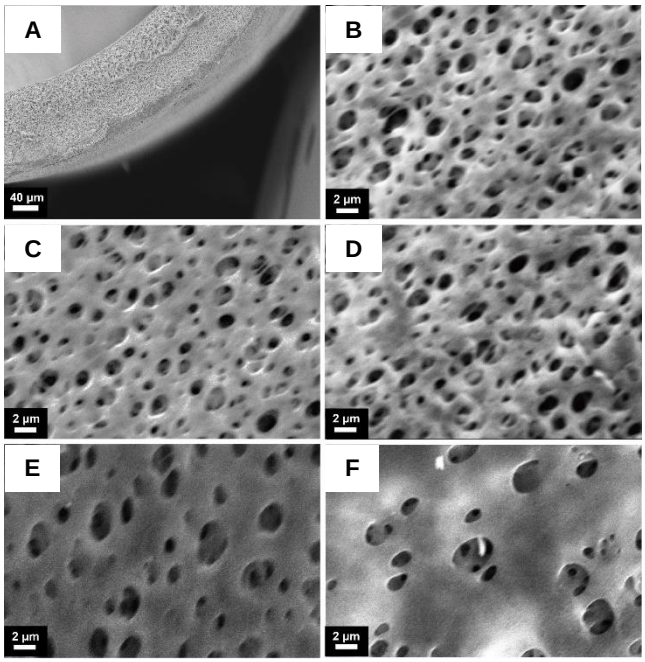

Figure 3. The FESEM images of pristine PES HF and SLGO coated PES HF membranes: (A) cross sectional SEM image of pristine PES HF; (B) surface SEM image of pristine PES HF; and surface SEM images of PES HF coated with (C) 1.55, (D) 3.10, (E) 6.20, and (F) 9.31 mg/m^2 of SLGO flakes.

The pore size distribution change with SLGO loading can further support the proposed deposition mechanism on PES HFs. Since SLGO flakes had a lateral size ranging from 0.7 to 1.3 µm, at small SLGO loading (1.55 mg/m^2), most of the SLGO flakes entered large pores, and only pores smaller than the size of SLGO flakes could be covered (Figure S3). Accordingly, the surface hydrophilicity of SLGO coated HF was not expected to be improved significantly due to the insufficient coverage of membrane surface. With the increase of SLGO loading (> 3.1 mg/m^2), most of small and medium pores were covered, and the edge of large pores started to be coated by SLGO flakes as well. At this stage of coating, SLGO deposited PES HF is expected to have a uniform coating layer, which could balance the surface hydrophilicity and transport resistance and thus reduce membrane fouling while keeping high permeance. However, after

passing this optimal point, increase of the GO loading (9.10 mg/m^2) raised the coating layer thickness and covered more large pores, leading to decreased permeance of membrane.

Addition to membrane surface hydrophilicity, surface roughness is another important property related with membrane fouling; usually, rougher membrane surface is more susceptible to fouling and more difficult to clean [15, 31]. To study the surface roughness change with SLGO loading, AFM was conducted to scan the surface of PES HF before and after SLGO coating. Figure 4 shows that as the SLGO loading increased from 1.55 to 6.20 mg/m^2, the surface of PES HF became smoother, and the surface roughness gradually reduced from 44 to 33 nm (Table 3), which is in a good agreement with the FESEM and pore size distribution results that most of the surface pores (small and medium size) were covered by SLGO flakes. However, when 9.31 mg/m^2 SLGO deposited on PES HF, the increased surface roughness was simply due to the over loading of SLGO on the membrane surface. Figure 4F exhibits the AFM image of a selected area where one SLGO flake was clearly scanned, indicating that SLGO flakes can completely conceal small/medium pores and partially cover big pore. Figure S4 also shows the 2D AFM images of UV-treated membranes. Comparison between PES_GO$_{6.20}$ and that with UV-treatment shows that surface roughness increased after UV-treatment. UV-treatment can create big holes on GO flakes, which cause the increase of the surface roughness. After 1.5 UV-treatment, surface roughness slightly decreased from 43 to 41 nm, probably resulting from the smaller GO flakes after UV irradiation[19].

Table 3. Surface roughness of pristine HF and SLGO coated PES HF membranes.

Membrane	Ra (nm)	Rms (nm)
PES	44.2	54.0
PES_GO$_{1.55}$	40.9	51.4
PES_GO$_{3.10}$	39.2	48.0
PES_GO$_{6.20}$	33.1	38.1
PES_GO$_{9.31}$	38.2	47.5
PES_GO$_{6.20}$_UV$_{0.5}$	34.2	39.4
PES_GO$_{6.20}$_UV$_{1.0}$	38.4	42.6
PES_GO$_{6.20}$_UV$_{1.5}$	37.8	41.7

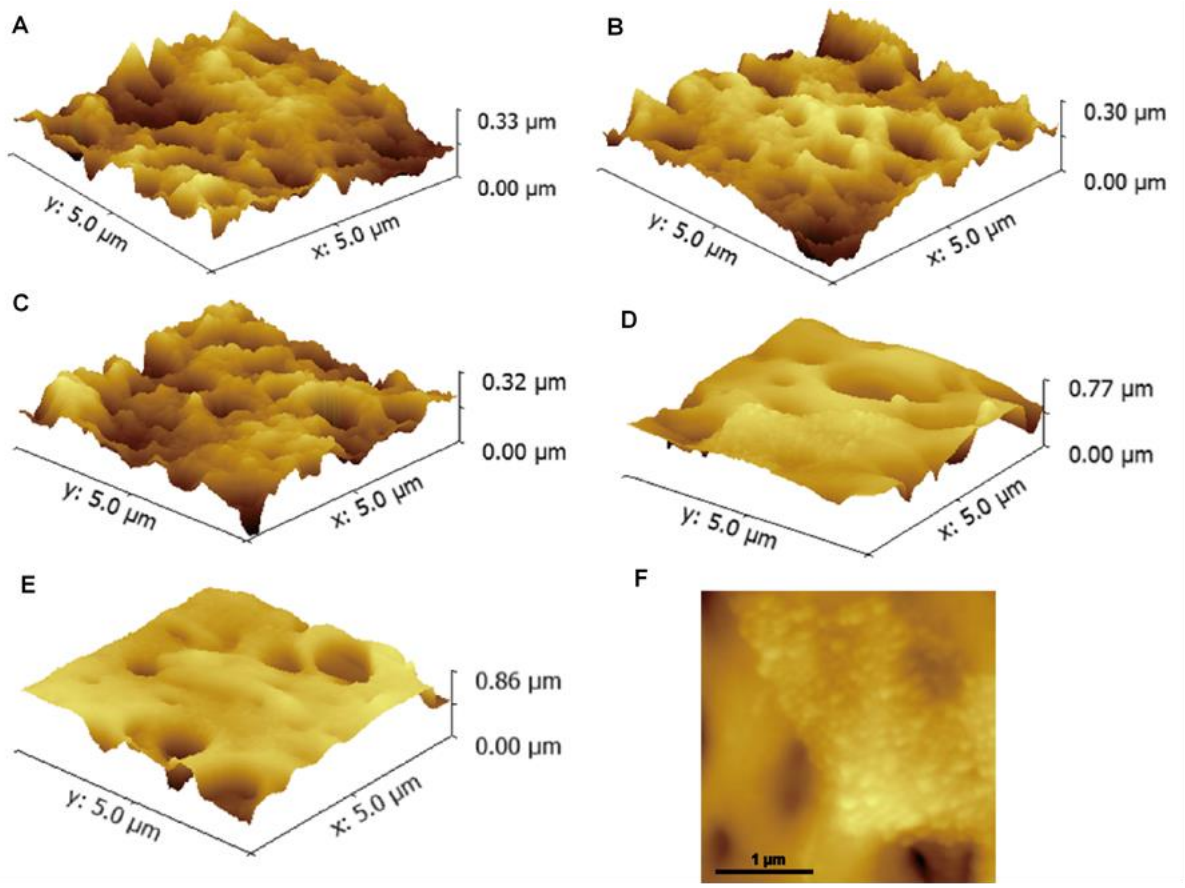

Figure 4. AFM topological scan of pristine PES HF and SLGO coated PES HF membranes: (A) 3D AFM image of pristine PES HF; (B)-(E) 3D AFM images of PES HF coated with 1.55, 3.10, 6.20, and 9.31 mg/m^2 of SLGO flakes, respectively; (F) AFM image of GO flake covered on PES HF surface and pores (PES_GO$_{6.20}$ Membrane).

3.2 Effect of SLGO coating on pure water permeation and antifouling performance

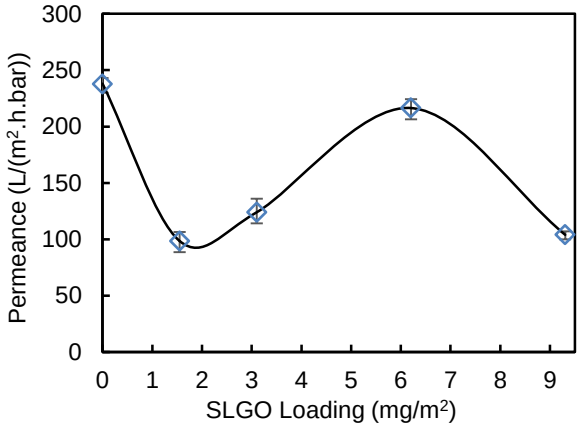

Figure 5. Pure water permeance of pristine PES HF and PES HF membranes deposited with different SLGO loading.

High permeance and good antifouling performance are two desired properties for membranes used in MBR applications. Therefore, the effect of SLGO loading on pure water permeation and antifouling performance of PES HF membranes were investigated. Pure water permeance of uncoated PES HF and SLGO deposited PES HF membranes was shown in Figure 5. With the increase of SLGO loading, water permeance decreased initially and then increased with SLGO loading; as more than 6.20 mg/m^2 of SLGO was deposited on PES HFs, the water permeance of membrane went back down again. Combined effect of two factors, surface hydrophilicity and transport resistance, could be used to explain the water permeation performance of SLGO coated PES HF membranes [5, 27, 32, 33]. When SLGO loading was low, such as 1.55 mg/m^2, surface hydrophilicity was not improved significantly enough to balance the transport resistance generated by the covering of small PES HF pores (mechanism explained in 3.1), therefore leading to a decrease of water permeance from 243 to 98 L(m^2·h·bar). By further increasing SLGO loading to 3.10 and 6.20 mg/m^2, improved surface hydrophilicity gradually dominated the water transport in PES HF membranes, and water permeance started to raise up. However, as SLGO loading increased to 9.31 mg/m^2, the surface hydrophilicity could not make up the greatly increased transport resistance, and thus the water permeance decreased. Therefore, 6.20 mg/m^2 of SLGO coating seems to be the optimum point where the surface hydrophilicity and transport resistance could be effectively balanced.

During the membrane separation process, membrane fouling is unavoidable, and foulant particles could stick on membrane surface, block pores and leading to the loss of permeance. However, a layer of GO coating could mitigate the adhesion of foulants to the membrane surface and thus improve membrane antifouling ability. Therefore, the antifouling performance of SLGO coated PES HF membranes was firstly investigated using three model foulants: SiO_2 particles, BSA, and sodium alginate (Figure 6). When using SiO_2 particles as the model foulant, the permeance of pristine PES HF decreased ~55% during the filtration test, while the maximum permeance drop for SLGO coated HF membranes was only around 25%. Similar trend was observed in filtration tests using BSA and sodium alginate as foulants. As shown in Figure 6, by testing all three model foulants, PES_$GO_{6.20}$ membrane coated with 6.20 mg/m^2 of SLGO exhibited the highest permeance over the whole filtration period, apparently resulting from its well-balanced surface hydrophilicity and transport resistance (as discussed above). After 4 h of fouling test, the permeance measured for PES_$GO_{6.20}$ membrane was 32, 40 and 18% higher than the pristine PES HF while using SiO_2 particles, BSA and sodium alginate as foulants, respectively.

3.3 UV-treatment on SLGO to improved antifouling performance of membranes

In an attempt to further improve the antifouling performance, we conducted UV treatment on SLGO flakes before coating on PES HFs. According to the previous study in our group, UV-irradiation could introduce extra hydrophilic functional groups, such as carboxyl or hydroxyl groups, onto GO flakes [18, 22, 29]. Therefore, by depositing UV-treated SLGO on PES HFs, the additional hydrophilic functional groups on GO flakes could increase the overall hydrophilicity of as-prepared PES HF membranes, and thus further improve the

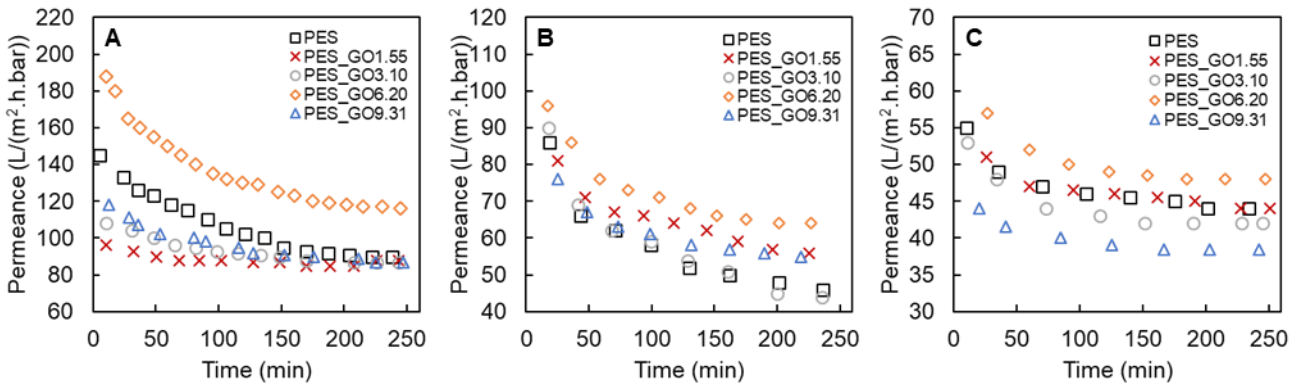

Figure 6. The antifouling performance of SLGO coated PES hollow membranes with using A) SiO_2 particles, B) BSA, and C) Sodium Alginate as model foulants.

antifouling ability. Here in, we prepared PES HF membranes coated with SLGO flakes treated by UV light for different durations (0.5 to 1.5 h), and the UV-treated SLGO loading was fixed to 6.20 mg/m^2. The effect of UV-treatment duration on the antifouling performance of as-prepared membranes were studied by fouling tests with the presence of the above three model foulants. As shown in Figure 7, the antifouling ability of PES HF membranes was significantly improved while being coated with UV-irradiated SLGO flakes.

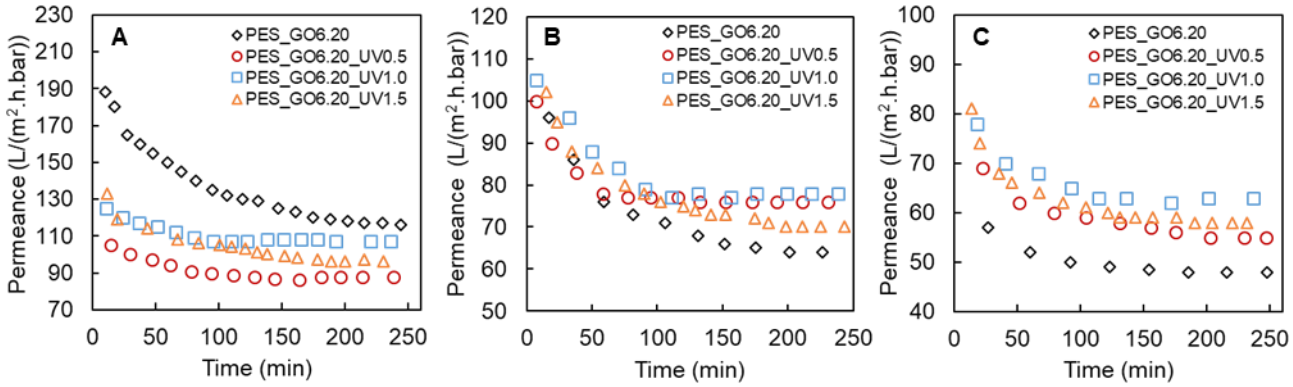

Figure 7. The antifouling performance of PES hollow membranes while using A) SiO_2 particles, B) BSA, and C) Sodium Alginate as model foulants. Membranes were coated with SLGO flakes irradiated by different duration of UV-treatment.

When using SiO_2 particles as the model foulant, the permeance of PES_GO$_{6.20}$ membrane dropped around 30% during the filtration test. In contrast, the membranes deposited with UV-treated SLGO had lower initial permeance, which might be due to the accumulation of SiO_2 on the membrane surface, but the permeance decreased less than 15% (PES_GO$_{6.20}$_UV$_{1.0}$) for the whole testing process. Similar improvements were also observed when using BSA and sodium alginate as foulants. Moreover, when running the fouling test with BSA and sodium alginate, PES HF membranes coated with UV-treated SLGO exhibited higher permeance, as shown in Figure 7C; the permeance significantly increased from 54 L/(m^2·h·bar) to 65 L/(m^2·h·bar) when the membrane was coated with 1 h UV-treated SLGO flakes (PES_GO$_{6.20}$_UV$_{1.0}$). Overall, by comparing the antifouling ability of all the UV-treated membranes, membrane PES_GO$_{6.20}$_UV$_{1.0}$ deposited with 6.20 mg/m^2 of 1h UV-treated SLGO exhibited the best performance among other samples.

PES_GO$_{6.20}$_UV$_{1.0}$ HF membrane and the pristine PES HF were selected for the long-term antifouling test in MBR while using activated sludge supplied by the City's Metropolitan Wastewater Treatment Plant (Columbia, SC, USA). Figure 8A shows that the permeate total organic carbon (TOC) concentration of pristine PES HF and PES_GO$_{6.20}$_UV$_{1.0}$ HF membrane was between 12 and 23 ppm, which means the rejection for oxidized carbon is more than 99%, demonstrating good separation performance of both PES HF and PES_GO$_{6.20}$_UV$_{1.0}$ HF membranes. However, the trans-membrane pressure of pristine PES HF increased faster at fixed permeate flux of 20 L/(m^2·h). As illustrated in Figure 8B, the trans-membrane pressure of PES HF drastically increased from 0.2 to 0.3 bar in the first 2 h, and then pressure increasement, from 0.3 to around 0.7 bar, gradually slowdown in the next 50 h. In contrast, in the very first stage, it took about 6 h to increase the trans-membrane pressure of the PES_GO$_{6.20}$_UV$_{1.0}$ membrane from 0.15 to 0.28 bar, and then the pressure slowly increased to 0.5 bar in 140 h, suggesting greatly improved antifouling performance of this membrane.

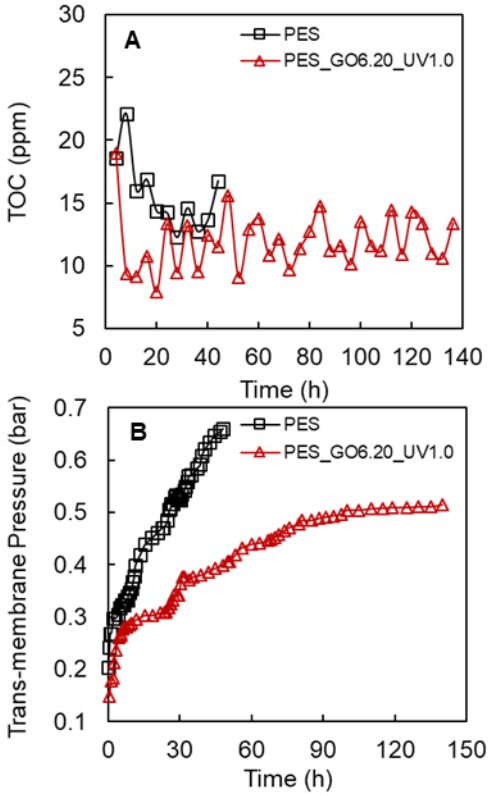

Figure 8. Long term fouling test of pristine PES and PES_GO$_{6.20}$_UV$_{1.0}$ hollow fiber membranes in MBR reactor: (A) change of total organic carbon concentration in the permeate of MBR with operation time; (B) the change of trans-membrane pressure with operation time.

Membrane surface morphology change after test in MBR was also examined by FESEM. As shown in Figure 9A, the foulant layer has

blocked most of the surface pores of the pristine PES HF, leaving only negligible number of open pores for permeation. In contrast, PES_$GO_{6.20}$_$UV_{1.0}$ membrane surface had negligible amount of foulant, and most of the surface pores were still open for permeation (Figure 9B). This result is consistent with the excellent filtration performance of PES_$GO_{6.20}$_$UV_{1.0}$ in MBR operation. The long-term MBR performance and FESEM images again confirmed that this UV-treated SLGO PES HF membrane could efficiently mitigate membrane fouling.

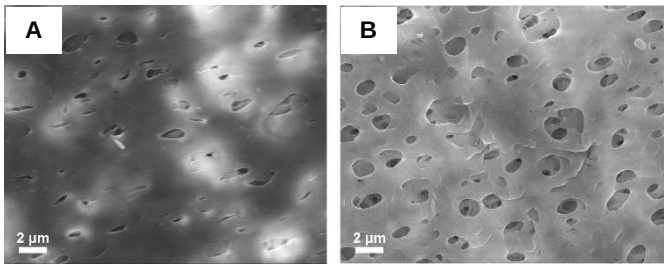

Figure 9. The FESEM image of fouled membrane after using in the MBR: (A) pristine PES HF after 2 days using in MBR reactor; (B) PES_$GO_{6.20}$_$UV_{1.0}$ HF membranes after 6 days using in MBR reactor.

4.0 Conclusion

In this work, ultrathin SLGO deposited PES HF membranes were fabricated via vacuum filtration method and used for MBR application. By using this facial vacuum filtration method, the PES HF surface can be selectively modified. Comparing with other methods [27, 28], the membrane permeance and antifouling performance was significantly improved with only small amount of SLGO loading, and the optimal SLGO loading was determined to be 6.20 mg/m^2. To further increase membrane hydrophilicity, UV-treated SLGO flakes was deposited on PES HFs; the PES_$GO_{6.20}$_$UV_{1.0}$ membrane, coated with 6.20 mg/m^2 of one hour UV-treated SLGO, exhibited excellent performance with high water permeance of 65 L/(m^2·h·bar) and the lowest fouling problem (<15% permeance reduction). Long time MBR filtration test was conducted to compare the stable separation performance of PES HF and PES_$GO_{6.20}$_$UV_{1.0}$ membrane for real waste water treatment. Trans-membrane pressure for pristine PES HF significantly increased to 0.7 bar after 50 h of testing. For PES_$GO_{6.20}$_$UV_{1.0}$ membrane, the trans-membrane pressure slowly raised to around 0.5 bar and then a stable pressure was maintained for 150 h with similar rejection, suggesting UV-treated SLGO coating can not only lead to improved membrane filtration performance, but also increase energy efficiency and reduce operation cost.

Conflict of interest

The authors declare no competing financial interest.

Acknowledgment

We gratefully acknowledge the support by National Science Foundation (NSF) Career Award under Grant No. 1451887.

References

1. G. T. Daigger, B. E. Rittmann, S. Adham and G. Andreottola, Are membrane bioreactors ready for widespread application?, *Environ. Sci. Technol.*, 2005, **39**, 399a-406a.

2. X. Huang, C. H. Wei and K. C. Yu, Mechanism of membrane fouling control by suspended carriers in a submerged membrane bioreactor, *J. Membr. Sci.*, 2008, **309**, 7-16.

3. I. S. Kim and N. Jang, The effect of calcium on the membrane biofouling in the membrane bioreactor (MBR), *Water Res.*, 2006, **40**, 2756-2764.

4. I. Sadeghi, P. Kaner and A. Asatekin, Controlling and Expanding the Selectivity of Filtration Membranes, *Chem. Mater.*, 2018, **30**, 21, 7328-7354.

5. I. Sadeghi, A. Aroujalian, A. Raisi, M. Fathizadeh and B. Dabir, Effect of solvent, hydrophilic additives and corona treatment on performance of polyethersulfone UF membranes for oil/water separation, *Procedia Eng.*, 2012, **44**, 1539-1541.

6. Y. N. Yang, H. X. Zhang, P. Wang, Q. Z. Zheng and J. Li, The influence of nano-sized TiO2 fillers on the morphologies and properties of PSFUF membrane, *J. Membr. Sci.*, 2007, **288**, 231-238.

7. S. Zinadini, A. A. Zinatizadeh, M. Rahimi, V. Vatanpour and H. Zangeneh, Preparation of a novel antifouling mixed matrix PES membrane by embedding graphene oxide nanoplates, *J. Memb. Sci.*, 2014, **453**, 292-301.

8. E. Celik, H. Park, H. Choi and H. Choi, Carbon nanotube blended polyethersulfone membranes for fouling control in water treatment, *Water Res.*, 2011, **45**, 274-282.

9. J. H. Choi, J. Jegal and W. N. Kim, Fabrication and characterization of multi-walled carbon nanotubes/polymer blend membranes, *J. Membr. Sci.*, 2006, **284**, 406-415.

10. K. Masoudnia, A. Raisi, A. Aroujalian and M. Fathizadeh, A hybrid microfiltration/ultrafiltration membrane process for treatment of oily wastewater, *Desalin. Water Treat.*, 2015, **55**, 901-912.

11. V. Vatanpour, S. S. Madaeni, A. R. Khataee, E. Salehi, S. Zinadini and H. A. Monfared, TiO2 embedded mixed matrix PES nanocomposite membranes: Influence of different sizes and types of nanoparticles on antifouling and performance, *Desalination*, 2012, **292**, 19-29.

12. M. H. Gu, J. E. Kilduff and G. Belfort, High throughput atmospheric pressure plasma-induced graft polymerization for identifying protein-resistant surfaces, *Biomaterials*, 2012, **33**, 1261-1270.

13. J. Huang, K. S. Zhang, K. Wang, Z. L. Xie, B. Ladewig and H. T. Wang, Fabrication of polyethersulfone-mesoporous silica nanocomposite ultrafiltration membranes with antifouling properties, *J. Membr. Sci.*, 2012, **423**, 362-370.

14. R. Z. Pang, X. Li, J. S. Li, Z. Y. Lu, X. Y. Sun and L. J. Wang, Preparation and characterization of ZrO2/PES hybrid ultrafiltration membrane with uniform ZrO2 nanoparticles, *Desalination*, 2014, **332**, 60-66.

15. I. Sadeghi, A. Aroujalian, A. Raisi, B. Dabir and M. Fathizadeh, Surface modification of polyethersulfone ultrafiltration membranes by corona air plasma for separation of oil/water emulsions, *J. Membr. Sci.*, 2013, **430**, 24-36.

16. I. Sadeghi, J. Kronenberg and A. Asatekin, Selective Transport through Membranes with Charged Nanochannels Formed by Scalable Self-Assembly of Random Copolymer Micelles, *Acs Nano*, 2018, **12**, 95-108.

17. I. Sadeghi, H. Yi and A. Asatekin, A Method for Manufacturing Membranes with Ultrathin Hydrogel Selective Layers for Protein Purification: Interfacially Initiated Free Radical Polymerization (IIFRP), *Chem. Mater.*, 2018, **30**, 1265-1276.

18. Y. Huang, H. Li, L. Wang, Y. L. Qiao, C. B. Tang, C. I. Jung, Y. M. Yoon, S. G. Li and M. Yu, Ultrafiltration Membranes with Structure-Optimized Graphene-Oxide Coatings for Antifouling Oil/Water Separation, *Adv. Mater. Interfaces*, 2015, **2**, 1400433.

19. K. Masoudnia, A. Raisi, A. Aroujalian and M. Fathizadeh, Treatment of Oily Wastewaters Using the Microfiltration Process: Effect of Operating Parameters and Membrane Fouling Study, *Sep. Sci. Technol.*, 2013, **48**, 1544-1555.

20. M. Fathizadeh, H. N. Tien, K. Khivantsev, J. T. Chen and M. Yu, Printing ultrathin graphene oxide nanofiltration membranes for water purification, *J. Mater. Chem. A*, 2017, **5**, 20860-20866.

21. M. Fathizadeh, W. W. L. Xu, F. L. Zhou, Y. Yoon and M. Yu, Graphene Oxide: A Novel 2-Dimensional Material in Membrane Separation for Water Purification, *Adv. Mater. Interfaces*, 2017, **4**.

22. F. L. Zhou, M. Fathizadeh and M. Yu, Single- to Few-Layered, Graphene-Based Separation Membranes, *Annu. Rev. Chem. Biomol.*, 2018, **9**, 17-39.

23. F. L. Zhou, H. N. Tien, W. W. L. Xu, J. T. Chen, Q. L. Liu, E. Hicks, M. Fathizadeh, S. G. Li and M. Yu, Ultrathin graphene oxide-based hollow fiber membranes with brush-like CO2-philic agent for highly efficient CO2 capture, *Nat. Commun.*, 2017, **8**.

24. W. L. W. Xu, F. L. Zhou and M. Yu, Tuning Water Nanofiltration Performance of Few-Layered, Reduced Graphene Oxide Membranes by Oxygen Plasma, *Ind. Eng. Chem. Res.*, 2018, **57**, 16103-16109.

25. W. W. L. Xu, C. Fang, F. L. Zhou, Z. N. Song, Q. L. Liu, R. Qiao and M. Yu, Self-Assembly: A Facile Way of Forming Ultrathin, High-Performance Graphene Oxide Membranes for Water Purification, *Nano Lett.*, 2017, **17**, 2928-2933.

26. Y. Z. Qin, Y. Y. Hu, S. Koehler, L. H. Cai, J. J. Wen, X. J. Tan, W. W. L. Xu, Q. Sheng, X. Hou, J. M. Xue, M. Yu and D. Weitz, Ultrafast Nanofiltration through Large-Area Single-Layered Graphene Membranes, *Acs Appl. Mater. Inter.*, 2017, **9**, 9239-9244.

27. J. Lee, H. R. Chae, Y. J. Won, K. Lee, C. H. Lee, H. H. Lee, I. C. Kim and J. M. Lee, Graphene oxide nanoplatelets composite membrane with hydrophilic and antifouling properties for wastewater treatment, *J. Membr. Sci.*, 2013, **448**, 223-230.

28. F. M. Jin, W. Lv, C. Zhang, Z. J. Li, R. X. Su, W. Qi, Q. H. Yang and Z. M. He, High-performance ultrafiltration membranes based on polyethersulfone-graphene oxide composites, *Rsc Adv.*, 2013, **3**, 21394-21397.

29. H. Li, Y. Huang, Y. T. Mao, W. W. L. Xu, H. J. Ploehn and M. Yu, Tuning the underwater oleophobicity of graphene oxide coatings via UV irradiation, *Chem. Commun.*, 2014, **50**, 9849-9851.

30. B. K. Hwang, W. N. Lee, K. M. Yeon, P. K. Park, C. H. Lee, I. S. Chang, A. Drews and M. Kraume, Correlating TMP increases with microbial characteristics in the bio-cake on the membrane surface in a membrane bioreactor, *Environ. Sci. Technol.*, 2008, **42**, 3963-3968.

31. I. Sadeghi, P. Arbab, M. Fathizadeh, H. Fakhraee and M. Amrollahi, Optimization of Nano-TiO2 Photocatalytic Reactor for Organophosphorus Degradation, *Adv. Mater. Sci. Eng.*, 2012, DOI: Artn 51012310.1155/2012/510123.

32. K. H. Chu, M. Fathizadeh, M. Yu, J. R. V. Flora, A. Jang, M. Jang, C. M. Park, S. S. Yoo, N. Her and Y. Yoon, Evaluation of Removal Mechanisms in a Graphene Oxide-Coated Ceramic Ultrafiltration Membrane for Retention of Natural Organic Matter, Pharmaceuticals, and Inorganic Salts, *Acs. Appl. Mater. Inter.*, 2017, **9**, 40369-40377.

33. M. Fathizadeh, H. N. Tein, K. Khivantsev, Z. Song, F. Zhou and M. YU, Polyamide/nitrogen-doped graphene oxide quantum dots (N-GOQD) thin film nanocomposite reverse osmosis membranes for high flux desalination, *Desalination*, 2019, **451**, 125-132.

34. F. Zhou, H.N. Tien, Q. Dong, W.L. Xu, H. Li, S. Li, and M. Yu, Ultrathin, ethylenediamine-functionalized graphene oxide membranes on hollow fibers for CO_2 capture, *J. Membr. Sci.*, 2019, **573**, 184-191

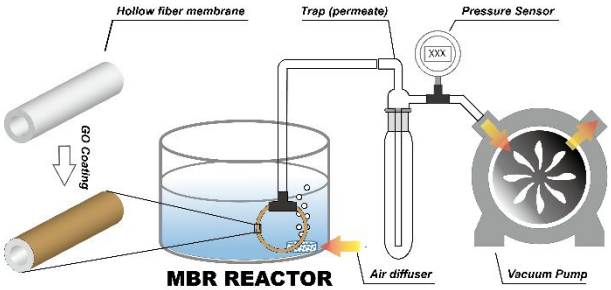

Single layer graphene oxide was studied as novel coating material to improve antifouling performance of PES HF membrane in MBR application.